Wetlands (2024) 44:51
https://doi.org/10.1007/s13157-024-01807-6

ORIGINAL RESEARCH ARTICLE

Examination of Drone Usage in Estimating Hardwood Plantations Structural Metrics

Tyler Corbin[1] · Mohammad Bataineh[2]

Received: 26 August 2023 / Accepted: 16 April 2024

Abstract

Planting hardwood trees on retired marginal agricultural land is one of the main strategies used to restore forested wetlands. Evaluating effectiveness of wetland restoration requires efficient monitoring to evaluate recovery trajectories and desired conditions. Recent advancements in unmanned aerial system (UAS) technologies have prompted wide-scale adoption of UAS platforms in providing a range of ecological data. In this study, we examined the use of UAS Structure from Motion (SfM) derived point clouds in estimating tree density, canopy height, and percent canopy cover for bottomland hardwood plantations within four wetland reserve easements. Using a local maxima approach for individual tree detection produced plantation level estimates with mean absolute errors of 150 trees per hectare, 0.5 m, and 18.4% for tree density, canopy height, and percent canopy cover, respectively. At the plot level, UAS-derived tree counts ($r = 0.53$, $p < 0.01$) and canopy height ($r = 0.57$, $p < 0.01$) were significantly correlated with ground-based estimates. We demonstrate that UAS-SfM is a viable method of assessing bottomland hardwood plantations for applications that require precision levels congruent with the mean absolute errors reported here. The accuracy of tree density estimates was reliant upon specific local maxima window parameters relative to stand conditions. Therefore, acquisition of leaf-off and leaf-on imagery may allow for better individual tree detection and subsequently more accurate tree density and other structural attributes.

Keywords Unmanned aerial system · Bottomland hardwood · Wetlands · Reserve easements · Restoration · Point clouds

Introduction

Bottomland hardwood forests within the Lower Mississippi Alluvial Valley originally covered 10 million ha, of which a third remains (King and Keeland 1999). Land use changes to agriculture and development as well as alteration of hydrology for flood control were lead contributors of bottomland hardwood forest loss (King and Keeland 1999; Klimas et al. 2009; Steven et al. 2015). Restoration of these forested wetlands is of high priority to support a wide range of benefits including improved habitat for migratory birds and forest-dependent wildlife, enhanced biodiversity and carbon sequestration, and maintenance of wetland function (Walbridge 1993).

The Agricultural Conservation Easement Program (ACEP) aims to provide financial incentives to protect agricultural viability and restore and enhance wetlands on eligible lands. The Wetland Reserve Easements (WRE) component of ACEP and its predecessor program, Wetlands Reserve Program (WRP), voluntarily enrolled 1.2 million ha nationwide since 1990 (NRCS 2023). In Arkansas alone, 106 727 ha were enrolled between 1995 and 2021. Afforestation of former agricultural land requires monitoring of planting survival, composition, and tree density as well as vegetation diversity and other structural metrics such as canopy cover and canopy height to evaluate recovery rates and achievement of desired conditions reflecting habitat suitability for migratory birds and threatened and endangered species (LMVJV et al. 2007; Berkowitz 2013). For example, ground-derived canopy cover higher than 90% is considered

✉ Mohammad Bataineh
mohammad.bataineh@usda.gov

[1] College of Forestry, Agriculture, and Natural Resources, University of Arkansas at Monticello, 110 University Court, 716561 Monticello, AR, USA

[2] Southern Research Station, Forest Service, United States Department of Agriculture, 2500 Shreveport Highway, 71360 Pineville, LA, USA

a management-warranting condition, while cover between 60 and 80% is considered within the desired target range for wetland reserve easements. The trajectories of bottomland hardwood forests restored under these programs will largely depend upon the ability of resource managers to monitor stand conditions and implement adaptive management strategies. The efforts of federal and state agencies along with private organizations to conduct post-restoration monitoring, however, are often constrained by a lack of time and financial resources (Berkowitz 2013). As thousands of hectares of bottomland hardwood forests continue to be restored each year, the need for a reliable, resource-efficient method of assessing stand structure is increasing.

Advancements in unmanned aerial system (UAS) technologies such as programmable flight patterns, improved accuracy of onboard positioning systems, lower prices, and increased options for onboard sensors have prompted wide-scale adoption of UAS platforms in the acquisition of a range of ecological data (Marcaccio et al. 2015). Compared to other platforms used for remote sensing such as satellites and manned aircrafts, UAS platforms are often more cost efficient at smaller spatial scales (< 500 ha) and offer increased spatial and temporal flexibility (Tao et al. 2011; Marcaccio et al. 2015; Maturbongs et al. 2019). As an alternative to ground-based forest inventory methods, remotely sensed data collected from UAS platforms have demonstrated potential to provide estimates of forest structural attributes (e.g., tree height and crown diameter), often requiring relatively lower investments of time and resources (Nasiri et al. 2021).

One method of capturing the three-dimensional structure of forest stands from UAS platforms relies on structure-from-motion (SfM) photogrammetry. A SfM photogrammetry application defines matching features within multiple overlapping images, tracks the features across each image, and triangulates the relative x, y, and z positions for each identified feature. Ultimately, SfM application allows for the construction of high-resolution aboveground models and three-dimensional point clouds like those obtained from Light Detection and Ranging (LiDAR) scanners (Wallace et al. 2016; Iglhaut et al. 2019; Maturbongs et al. 2019). Though LiDAR allows for increased canopy penetration and often results in more detailed depiction of forest structure, previous studies suggest SfM generated point clouds using Red/Green/Blue (RGB) sensors remain an adequate low-cost alternative (Wallace et al. 2016).

Previous studies have assessed the potential of SfM generated point clouds to estimate forest structural metrics, such as canopy cover, height, and vertical profile (Wallace et al. 2016; Iglhaut et al. 2019), the accuracy of the derived forest metrics across forest types is not well-established, particularly for inventories conducted in deciduous forests, where crown geometry can be irregular and difficult to discern (Ke and Quackenbush 2011; Jayathunga et al. 2018). If accurate, a methodology to derive forest structural metrics using UAS imagery could provide agencies with the ability to assess forest conditions and monitor stand structure of WRP easements in a time and resource-efficient manner. To that end, this study aimed to examine the usage of UAS for estimating structural metrics of hardwood plantations. Specifically, this study: (1) used high resolution images collected from a UAS platform and structure-from-motion point cloud data to extract structural metrics of seven hardwood plantations within four WRP easements; and (2) assessed the accuracy of UAS-derived structural metrics using ground-based inventory data as a reference.

Materials and Methods

Study Site

The study was conducted within four WRP easements containing seven hardwood plantations across three Arkansas counties, Ashley; Desha; and White (Fig. 1). Easements were selected to represent the range of available conditions across a subset of the oldest WRP easements in Arkansas (closing dates prior to 2003) with respect to dominant tree species, basal area, and stand density. Easements were planted with red oaks such as: willow oak (*Quercus phellos*), Nuttall oak (*Q. texana*), cherrybark oak (*Q. pagoda*), and water oak (*Q. nigra*); white oaks such as: overcup oak (*Q. lyrata*) and swamp chestnut oak (*Q. michauxii*); and green ash (*Fraxinus pennsylvanica*). Volunteer recruitment from willow (*Salix* spp.), cottonwood (*Populus* spp.), sweetgum (*Liquidambar styraciflua*), American sycamore (*Platanus occidentalis*), and sugarberry (*Celtis laevigata*) also contributed to the species composition. Easements across the three sampled counties represented a gradient in species composition, with green ash and volunteer species dominating in Ashley County, red oaks dominating in Desha County, and a mixture of red oaks, green ash, and volunteer species occurring in White County. All easements were within the Mississippi Alluvial Plain Ecoregion, a highly altered system through land conversion to agriculture and urban use coupled with changes in hydrologic pattern through flood control projects during the 19th and 20th centuries (King and Keeland 1999). The largest concentration of bottomland hardwood forests occurred in this Ecoregion with only a third of the forested area (2.8 million ha) remaining by 1980s (King and Keeland 1999).

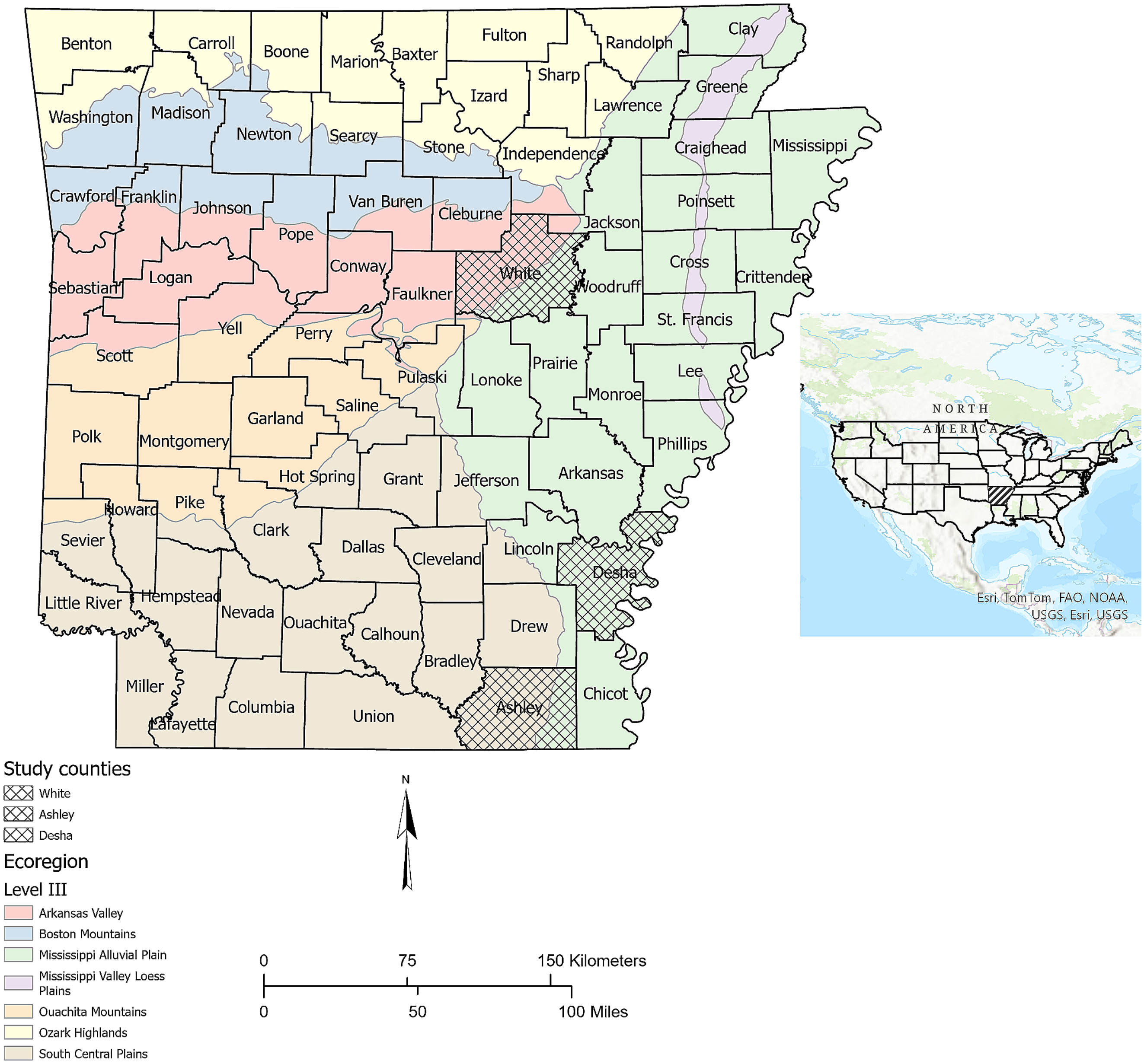

Fig. 1 Three Arkansas counties within the mississippi alluvial plain where four easements including seven plantations were sampled

Ground Data Collection

Ground-based inventory data used to assess the accuracy of UAS-derived structural metrics were collected in June and July 2018 using a series of concentric, nested, 0.04 ha circular plots. Within each planted field, sampling plots were established along linear transects across compositional and structural heterogeneity of field conditions. Linear transects represented a grid overlay across delineated plantations. Sampling transects were randomly selected for each plantation with plots placed at fixed 50 to 200 m intervals along each transect, with 9, 42, and 6 plots allocated to Ashley, Desha, and White easements, respectively (Table 1). Plot locations along each transect were determined by field conditions, with shorter spacing used for heterogeneous conditions (i.e., more plots) and larger spacing for homogenous conditions (i.e., fewer plots). Tree species, diameter at breast height (dbh) (cm), tree height (THT) (m), crown diameter (m), and crown density (%) were recorded for each live overstory tree with a dbh $\geq$ 7.6 cm. Tree height was measured using a hypsometer to the tallest live branch excluding dieback. Crown diameter was measured as the average horizontal distance for the crown's widest axis and its perpendicular axis to the nearest 0.1 m.

UAS Data Collection

Leaf-on imagery was collected using a 20-megapixel RGB senseFly Sensor Optimized for Drone Applications (SODA) onboard a senseFly eBee X UAS. The eBee X is a fixed-wing platform with a wingspan of 116 cm, maximum flight time of up to 90 min, and a maximum flight range of 55 km. The senseFly S.O.D.A. has a ground sampling resolution of 2.5 cm/px at 122 m above ground level (AGL). Positional, gyroscopic, and accelerometer data were collected during each flight using the onboard inertial measurement unit (IMU) (senseFly eBee X specifications).

UAS imagery was collected during leaf-on conditions in May and June of 2020 and 2021. Within each easement, plantation boundary shapefiles were used as fences in senseFly's eMotion® software for flight preparation. Flight altitudes, longitudinal image overlap, and lateral image overlap were set to 120 m (above ground level), 85%, and 75%, respectively. Flights were conducted in a grid pattern utilizing the perpendicular flight line option, to enable the UAS to make a second pass over the plantation.

A post-processing kinematic (PPK) workflow was used to further improve the accuracy of the positional data associated with each collected image. The PPK technique uses a static GNSS receiver as the base station to provide positional data from a known location. Data collected by the base station GNSS receiver is then georeferenced with the positional data collected by the onboard IMU to further improve the positional accuracy of each image. The PPK operation was conducted after each flight to replace the process of establishing ground control points (GCP). The accuracy of GCPs used for georeferencing of positional data depends on the number of points established as well as the spatial arrangement of the points (Tomaštík et al. 2019). The PPK technique, however, has been shown to provide accurate (within centimeters), consistent, and time-efficient structure from motion data (Tomaštík et al. 2019; Zhang et al. 2019). A Trimble R10 Model 2 survey-grade GNSS base station receiver referenced to the World Geodetic Datum of 1984 (WGS84) was used to collect static positional data within the Universal Transverse Mercator (UTM) coordinate system. Before each flight, the base station was placed in an open area near the delineated plantation to ensure adequate satellite coverage. Data logging was configured for continuous collection at 1 s intervals. Data logging was conducted for a minimum of 1 h for all flights. After flights were conducted, positional data collected from the Trimble R10 base station receiver were imported to eMotion® for post-processing.

Data Processing

Post-processed images were imported to PIX4Dmapper v.4.7.5 structure from motion (SfM) photogrammetry software to create a three-dimensional point cloud and orthomosaic imagery for each plantation. PIX4Dmapper utilizes an automated workflow consisting of initial image processing, point cloud densification, and orthomosaic creation. Additionally, version 4.7.5 allows for automatic classification of points within the point cloud using the American Society for Photogrammetry and Remote Sensing (ASPRS) standard classes (i.e., Ground, Low Vegetation, High Vegetation, Building, etc.). PIX4Dmapper then stores the constructed point cloud in LAS file formats containing X, Y, and Z positional attributes as well as assigned classes for each point. To meet photogrammetric processing requirements, a desktop PC equipped with an AMD Ryzen 9 5950×16-Core processor, 128GB RAM, 64-bit Windows OS, and NVIDIA RTX 3090 24GB GPU was used. Relevant photogrammetric processing outputs are summarized in Table 1.

Classified point clouds and orthomosaic tiles for each easement were imported to ArcGIS Pro (v.2.8.0). Point clouds were extracted within each delineated plantation boundary using the Extract LAS tool within the 3D Analyst toolbox. The resulting point clouds were then displayed over the corresponding orthomosaic images and filtered to

Table 1 Pix4dmapper photogrammetric processing output

County	Stand ID	N[a]	Images[b]	Flight Area (ha)	Average GSD[c] (cm)	Matched 2D-Key Points	3D-Points	MRE[d] (Pixels)
Ashley[e]	02_001	3	1132	118.9	3.0	2 155 874	752 071	0.12
Ashley[e]	02_002	3						
Ashley[e]	02_003	3						
Desha	07_011	21	681	64.4	2.8	1 786 791	798 334	0.12
Desha	07_012	9	545	58.5	2.8	805 697	343 992	0.11
Desha	10_001	12	554	85.2	2.8	186 885	75 403	0.09
White	25_006	6	685	37.7	2.8	1 584 371	639 082	0.12

[a] Number of ground plots

[b] Number of collected images

[c] Ground Sampling Distance

[d] Mean Reprojection Error

[e] One flight

display only ground-classified points. Manual reclassification of erroneously classified ground points was conducted by visually examining the orthomosaic images and overlaid point clouds, then reassigning the erroneously classified ground points to appropriate classes. Various degrees of manual ground point classification corrections were conducted across all PIX4D-classified point clouds. After ground point classification edits, LAS files were imported to RStudio and analyzed using the lidR (v.3.0.4) package (RCoreTeam 2023).

Data Analysis

To extract structural metrics, point clouds were subjected to three fundamental steps (Roussel et al. 2023): (1) height normalization, (2) creation of canopy height models, and (3) individual tree detection. Finally, UAS-SfM derived structural metrics were compared to traditional ground-based forest inventory metrics for each plantation using correlation and mean absolute error as an estimate of precision.

Height normalization refers to the process in which height values associated with each point representing elevation above mean sea level are converted to represent height above the ground (Roussel et al. 2023). Height normalization was required to facilitate the comparison of above ground vegetation heights. For each point cloud, points with elevation values below zero and duplicate points were removed prior to height normalization. Height normalization was conducted by interpolating ground point elevations using the k-nearest neighbor approach and inverse-distance weighting to subtract from non-ground points elevation. For point clouds of delineated plantations in which points were outside the convex hull area, digital terrain model (DTM) was used to subtract from non-ground points elevation.

Canopy height models (CHM) were constructed for each plantation using a point-to-raster algorithm (Roussel et al. 2023). In point-to-raster algorithms, the highest point in a normalized point cloud is attributed to each pixel in the CHM raster. Pixel size of CHM raster is user-defined and is generally a compromise between too fine of resolution that may result in voids or coarse resolution that may mask vegetation height differences. Plantations CHM were created using a fixed 1 m resolution that appeared to optimize voids vs. masking of height differences.

With a variety of algorithms and approaches available to perform individual tree detection (ITD), the local maxima (LM) technique is recognized as one of the simplest and most prominent ITD methods (Mohan et al. 2021). The LM algorithm detects and treats the highest point within a user defined window as a tree. The accuracy of ITD using LM algorithms is therefore ultimately influenced by the selected window parameters. ITD-LM detection is also influenced by tree species composition, overall forest structure, suboptimal window size and shape selection. All of which can result in the commission and/or omission of algorithm-defined treetops (Popescu and Wynne 2004). In general, optimizing window size and shape parameters for ITD in even-aged plantations is challenging, and the detection of deciduous trees has not been well studied (Gebreslasie et al. 2009; Ke and Quackenbush 2011). To evaluate the effect of window parameters on stand level tree density estimates, a LM algorithm was applied to the normalized point cloud and its rasterized CHM version for each plantation. Circular and square windows each at fixed sizes of 3 m, 5 m, and 7 m, respectively, were used. A variable window size function was also employed in which the window size increased linearly with higher point/pixel height (z value) for each square or circular window, using the notion that taller dominant hardwood trees tend to have larger crown diameters and larger area of influence.

For each combination of window shape (circular vs. square) and size (3 m, 5 m, and 7 m), tree density estimates were derived. Tree density estimates were derived at plantation and ground-inventory plot levels. At the plantation level, tree density was determined on a per hectare basis by dividing the number of detected trees by total stand area. Plot level tree density on a per hectare basis, was derived only from the normalized point cloud as counts of detected trees within a georeferenced area corresponding to ground-inventory plot locations. Mean absolute error in tree density estimates was calculated at plantation and plot levels as the average of absolute difference between point cloud and ground-inventory derived tree densities for each window shape and size combination. Most suitable window parameters were selected based on the lowest mean absolute error.

To extract canopy height and canopy cover metrics for each plantation, point clouds were segmented using the treetops identified using window parameters resulting in the lowest proportion of absolute difference between ground and UAS-derived metrics to ground-based measurements (i.e., relative error). Percent canopy cover was determined as the sum of detected individual tree crowns area in hectares divided by the plantation area. Individual tree crowns were delineated using convex polygons. Ground-based canopy cover was calculated as the proportion of the sum of individual overstory tree crown projection areas to pooled plot area. Average canopy height was calculated as the mean of overstory tree total heights pooled at the plantation and plot levels for ground measurements, while the mean of the maximum z value assigned to each detected treetop within the segmented point cloud was used to calculate mean canopy height representing the UAS-derived metric.

Results

Tree Density

The average tree density across all seven stands was 531 trees per hectare (215 trees per acre) based on ground inventory data (Table 2). For ITD performed on the normalized point cloud, the average number of trees detected across all stands was greatest using fixed, three-meter diameter, circular windows with an average of 427 trees per hectare (173 trees detected per acre), which is closest to the ground inventory. For individual tree detection performed on the canopy height model, the average number of trees detected across all stands was also greatest using fixed, three-meter diameter, circular windows, with an average of 363 trees per hectare (147 trees detected per acre), and the same average number of trees per acre was detected when using three-meter square windows. Additionally, ITD performed on the normalized point cloud using fixed, three-meter diameter, circular windows resulted in stand level tree density estimates with the lowest mean absolute error of 183 trees per hectare (74 trees per acre) when compared to ground-derived density estimates across all stands (Table 3).

The absolute errors of UAS-derived tree density estimates using three-meter, circular windows on the normalized point cloud ranged from 13 trees per hectare (five trees per acre) to 584 trees per hectare (236 trees per acre) using ground-derived density estimates as reference values (Table 4). For the same parameters, percent relative error, calculated as the absolute error as a proportion of ground-based tree density estimates, for each stand ranged from 2.9% (07_012) to 97.2% (10_001), with an average of 35.7% across all stands (Table 4). In general, higher absolute errors appeared to be associated with relatively dense stands (i.e., stands with ground-derived densities of 660 trees per hectare or more).

Spearman's rank correlation coefficient was used to assess the relationship between UAS-derived tree density estimates and ground-based estimates at the stand level (Table 5). None of the evaluated window parameter combinations produced tree density estimates that were significantly correlated with ground-based measurements, albeit 3 m windows had higher correlation coefficients than other window parameters. Thus, indicating weaker association between UAS-derived and ground-based tree density estimates as fixed window sizes increased regardless of window shape.

Using optimized window parameters (i.e., window shape and size combinations resulting in the lowest relative error) for each stand, the absolute errors of UAS-derived tree density estimates on the normalized point cloud ranged from three trees per hectare (one tree per acre) (02_002) to 584 trees per hectare (236 trees per acre) (25_006) compared

Table 2 Ground inventory derived structural metrics (mean ± standard error) for seven hardwood plantations within four Wetland Reserve Easements across three Arkansas counties

County	Stand ID	N[a]	Area (ha)[b]	Density ($trees.ha^{-1}$)	Basal Area ($m^2.ha^{-1}$)	QMD (cm)[c]	HT (m)[d]	Crown Diam. (m)[e]	Canopy Cover (%)
Ashley	02_001	3	10	667 ± 120	18.6 ± 6.0	18.2 ± 1.7	11.4 ± 0.4	4.5 ± 1.0	119 ± 25
Ashley	02_002	3	13	350 ± 164	4.0 ± 1.0	16.8 ± 5.4	9.7 ± 0.2	4.2 ± 0.9	53 ± 20
Ashley	02_003	3	12	708 ± 178	9.0 ± 3.1	12.3 ± 0.7	9.2 ± 0.3	3.5 ± 0.8	81 ± 22
Desha	07_011	21	21	361 ± 38	6.5 ± 0.8	14.9 ± 0.6	8.7 ± 0.1	4.3 ± 0.3	57 ± 7
Desha	07_012	9	26	444 ± 61	6.6 ± 0.8	14.0 ± 0.6	9.1 ± 0.1	4.7 ± 0.4	80 ± 10
Desha	10_001	12	27	178 ± 43	3.7 ± 0.8	14.1 ± 0.5	8.1 ± 0.2	4.7 ± 0.3	40 ± 9
White	25_006	6	17	1013 ± 208	17.1 ± 3.4	15.2 ± 1.6	13.2 ± 0.2	3.3 ± 0.5	101 ± 11

[a] Number of ground plots

[b] Plantation area

[c] Quadratic mean diameter

[d] Canopy height

[e] Crown diameter

Table 3 UAS-derived tree density using individual tree detection window shape and size parameters applied to a normalized point cloud (NLAS) vs. its rasterized version of Canopy Height Model (CHM)

ITD Method[a]	Window Size (m)	Window Shape	Detected Density (trees.ha^{-1})[b]	MAE (trees.ha^{-1})[c]
CHM	3	Circular	363	205
CHM	3	Square	363	205
CHM	5	Square	175	351
CHM	5	Circular	175	353
CHM	7	Circular	128	397
CHM	7	Square	104	422
CHM	Variable	Circular	324	237
CHM	Variable	Square	292	267
NLAS	3	Circular	427	183
NLAS	3	Square	353	209
NLAS	5	Circular	213	319
NLAS	5	Square	175	351
NLAS	7	Circular	128	398
NLAS	7	Square	101	423
NLAS	Variable	Circular	301	253
NLAS	Variable	Square	252	293

[a] Individual tree detection application to: a normalized point cloud (NLAS) vs. its rasterized Canopy Height Model (CHM) version

[b] Number of detected trees at plantation-level

[c] Mean absolute error

Table 4 UAS-derived tree density for hardwood plantations using individual tree detection applied to a normalized point cloud (NLAS) with a circular 3 m window

County	Stand ID	Detected Tree Count	Detected Density (trees.ha^{-1})[a]	Absolute Error (trees.ha^{-1})[b]	Relative Error (%)[c]
Ashley	02_001	4928	507	160	24.0
Ashley	02_002	5667	438	88	25.1
Ashley	02_003	5255	448	260	36.7
Desha	07_011	7758	383	22	6.1
Desha	07_012	11,341	431	13	2.9
Desha	10_001	9380	351	173	97.2
White	25_006	7292	429	584	57.7

[a] Number of detected trees at plantation-level

[b] Absolute difference between UAS-derived and ground-based density estimates

[c] Relative error is proportion of absolute error to ground-based density estimate

to ground-based tree density estimates (Table 6). Percent relative error using optimized window parameters for each stand ranged from 1% (02_002) to 57.7% (25_006), with an average of 19.1%, and a mean absolute error of 150 trees per hectare (61 trees per acre) across all stands.

Individual tree detection was conducted on the normalized point cloud at the plot level using the same window parameters as used for stand level metrics. Each window parameter combination was applied to all plots in each stand for a total of 60 plots. A comparison of the number of ground-based overstory trees per plot to UAS-derived estimates resulted in the mean absolute errors listed in Table 7. At the 0.04 ha plot level, MAE was lowest for circular

Table 5 Spearman's rank correlation coefficient (r) and p-values for UAS-derived and ground-based hardwood plantation tree density estimates for each of window shape and size parameter combinations

Window Shape	Window Size (m)	r	p
Circular	3	0.50	0.25
Circular	5	0.61	0.17
Circular	7	0.21	0.66
Circular	Variable	0.34	0.45
Square	3	0.68	0.11
Square	5	0.29	0.53
Square	7	-0.21	0.66
Square	Variable	0.43	0.35

Table 6 UAS-derived tree density for hardwood plantations using individual tree detection applied to a normalized point cloud (NLAS) and window parameters resulting in the lowest relative error as compared to ground-based density estimates

County	Stand ID[1]	Detected Density (trees.ha^{-1})[a]	Absolute Error (trees.ha^{-1})[c]	Relative Error (%)[d]
Ashley	02_001	507	160	24.0
Ashley	02_002[b]	353	3	1.0
Ashley	02_003	448	260	36.7
Desha	07_011	383	22	6.1
Desha	07_012	431	13	2.9
Desha	10_001[2]	168	10	5.6
White	25_006	429	584	57.7

[a] For all plantations except 02_002 and 10_001, circular 3 m windows were used

[b] Square 3 m and square 5 m windows were used for 02_002 and 10_001 plantations, respectively

[c] Absolute difference between UAS-derived and ground-based density estimates

[d] Relative error is proportion of absolute error to ground-based density estimate

Table 7 UAS-derived tree density for sampling plots using individual tree detection window shape and size parameters applied to a normalized point cloud (NLAS).

Window Shape	Window Size (m)	Detected Density (trees.ha^{-1})[a]	MAE (trees.ha^{-1})[b]
Circular	3	575	250
Circular	5	300	225
Circular	7	200	275
Circular	Variable	425	250
Square	3	475	225
Square	5	250	250
Square	7	175	300
Square	Variable	375	250

[a] Number of detected trees at ground inventory plot-level

[b] Mean absolute error

windows 5 m in diameter, followed by square windows 3 m in length. Although 5 m circular windows had the lowest MAE, values of MAE did not differ by more than 3 trees per plot (i.e., 25 to 75 trees per ha), with a range of 9 to 12 trees per plot (225 to 300 trees per ha). The average number of trees per plot measured on the ground across all stands was 17 trees (425 trees per ha).

Linear correlation between UAS-derived and ground-based tree counts at the sampling plot-level also decreased as fixed window size increased (Table 8). Overall, tree counts derived using fixed, three-meter circular, fixed, three-meter square, and fixed, five-meter circular windows were significantly correlated ($p<0.01$) with ground-based tree counts. Tree counts derived using fixed, three-meter circular windows, however, were more closely related to ground-based counts compared to tree counts derived using fixed, three-meter square windows and fixed, five-meter circular windows (Table 8).

Canopy Height

At the plantation level, UAS-derived canopy heights were highly correlated with ground-based measurements ($r=0.93$, $p<0.01$) using Spearman's correlation coefficient (Fig. 2a). Absolute errors associated with UAS-derived estimates of average canopy height ranged from 0.1 m (07_011) to 1.6 m (25_006), with an overall mean absolute error of 0.5 m across all stands. UAS-derived canopy height appeared to be slightly underestimated at plantation level, especially at the high end of canopy height range (Fig. 2a).

At the plot level, UAS-derived canopy heights were also significantly correlated with ground-based measurements ($r=0.57$, $p<0.01$) using Spearman's correlation coefficient (Fig. 2b). Absolute errors associated with UAS-derived estimates of canopy height ranged from 0.1 m to 8.2 m across sampling plots, with an overall mean absolute error of 1.4 m. Plot level UAS-derived canopy height was mainly underestimated in plots within highest tree density plantations (25_006), while overestimation was associated with plots of the third highest tree density plantations (02_001).

Table 8 Correlation coefficient (r) and p-values for the relationship between UAS-derived and ground-based sampling plot tree density estimates for each combination of window shape and size parameters

Window Shape	Window Size (m)	r[1]	p
Circular	3	0.53	<0.01
Circular	5	0.34	<0.01
Circular	7	0.27	0.04
Circular	Variable	0.15	0.26
Square	3	0.45	<0.01
Square	5	0.23	0.08
Square	7	0.19	0.15
Square	Variable	0.04	0.76

[1] Spearman's rank correlation coefficient

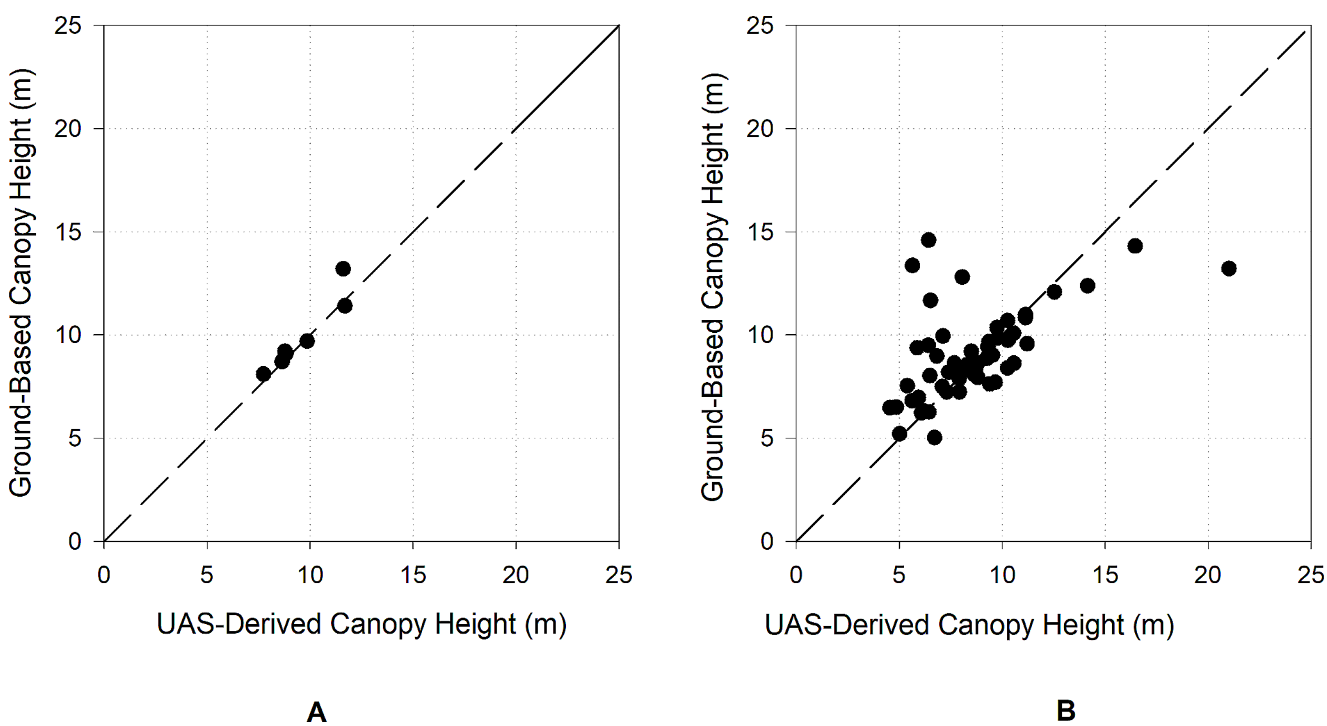

Fig. 2 A 1:1 graph of canopy height (m) obtained using ground measurements vs. UAS-derived segmented normalized point clouds pooled at: (**a**) Hardwood plantation level; and (**b**) Sampling plot level

Canopy Cover

UAS-derived canopy cover ($n=7$) estimates were significantly correlated ($r=0.82$, $p=0.03$) with ground-based measurements using Spearman's correlation coefficient (Fig. 3). Absolute error ranged from 2% (02_003) to 29% (02_001), with an overall mean absolute error of 18.4% across all stands. UAS-derived absolute error range was similar to standard error estimates for ground-derived canopy cover, which ranged from 7 to 25% (Table 2). Smallest UAS-derived absolute errors (02_003 and 25_006) were associated with smaller ground-derived crown diameters of 3.5 and 3.3 m, respectively (Table 2). UAS-derived canopy cover mainly overestimated ground-based canopy cover by 16.7% (Fig. 3). Overestimation of canopy cover for WRP plantations on the lower or upper end of target ranges may lead to misclassification of those plantations regarding meeting of target conditions or needs for management. Therefore, it is important to proceed cautiously when classifying plantations on the margins of target ranges using UAS-derived canopy cover. UAS-derived canopy cover estimates may also be down corrected to address overestimation compared to ground-derived canopy cover. Alternatively, UAS-derived canopy cover may be used to establish target ranges for defining desired conditions or target ranges.

Discussion

This study evaluated the potential of remotely sensed data collected from a UAS platform to assist resource managers in evaluating structural attributes of bottomland hardwood forested wetlands. While forest structure encompasses a suite of relevant metrics, we focused on stand level measurements of canopy height, canopy cover, and tree density for their utility in informing a variety of resource management and monitoring assessments, particularly for inventories conducted in deciduous forests, where crown geometry can be irregular and difficult to discern (Ke and Quackenbush 2011; Jayathunga et al. 2018).

Overall, UAS technologies offer the primary benefit of increased flexibility in temporal and spatial scales at which ecological data can be collected. Despite this benefit, key logistical and technical limitations to data acquisition still

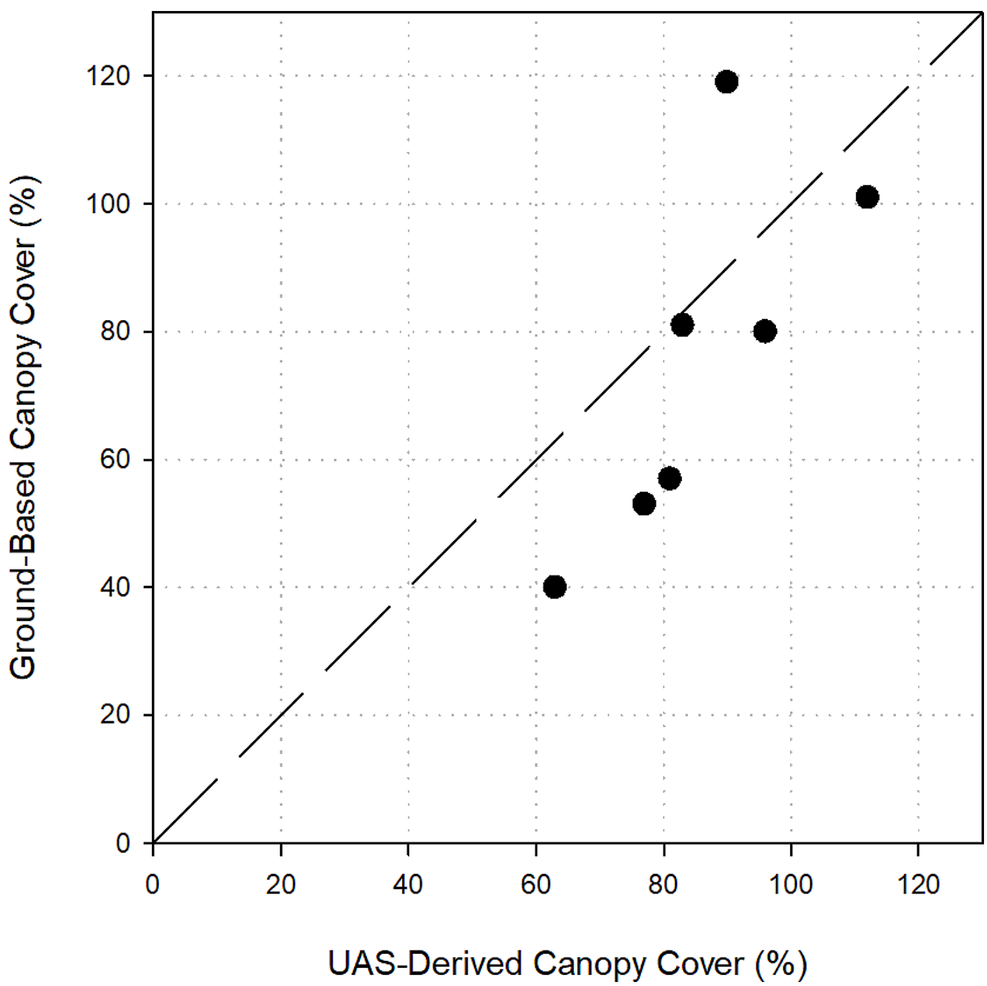

Fig. 3 A 1:1 graph of canopy cover (%) obtained using ground measurements vs. UAS-derived segmented normalized point clouds for seven Arkansas hardwood plantations enrolled in the Wetland Reserve Program

exist. Though the effects of extraneous variables on image or point cloud quality were not quantified, high wind speeds, precipitation, and cloud cover ultimately limited available days to fly. Additionally, flight parameters such as image overlap values and flight altitude influence image key point identification, ground-sampling distance, and density of obtained 3D point clouds. However, the greatest challenge was individual tree detection and segmentation.

Using a local maxima approach to identify individual treetops required the consideration of the influence of window size and shape on the quantity of trees detected per plantation. Of the various window parameters tested, fixed, 3 m circular windows employed on the normalized point clouds produced stand level tree density estimates with the lowest mean absolute error 175 trees per hectare (71 trees per acre) across all stands. Aside from the fact that it resulted in tree density estimates with the lowest mean absolute error across all stands, the decision to utilize the normalized point clouds instead of the two-dimensional, rasterized CHM's for deriving structural metrics was made due to the higher amount of detail provided by the three-dimensional format of the point clouds. After window parameters resulting in the lowest relative error for each stand were selected, overall mean absolute error across all stands was reduced to 150 trees per hectare (61 trees per acre). We selected the local maxima technique for individual tree detection due to its prominence and relative simplicity to employ. However, specific window size selection has not been optimized for bottomland hardwood forests and the automated detection of deciduous tree species, in general, has not been fully studied (Ke and Quackenbush 2011). Most examples of the local maxima approach to individual tree detection primarily come from coniferous stands in which regularity in crown shape and apical dominance facilitate a more accurate detection of local maxima (Zhen et al. 2016). In addition to species composition, overall forest structural attributes such as tree density and canopy cover influence individual tree detection accuracy (Falkowski et al. 2008). Higher individual tree detection accuracy is often associated with relatively open canopy conditions, whereas lower accuracy is often associated with closed canopy conditions (Falkowski et al. 2008). As is the case with many wetland reserve easements, high tree densities, irregularity in crown shape, and crown overlap likely contributed to the inaccuracies of our UAS-derived tree density estimates. For instance, using window parameters with the lowest relative error for each plantation, the largest errors in individual tree detection were associated with stands having the highest tree densities, tree species diversity, and percent canopy cover (02_001, 02_003, and 25_006) (Table 2). For the same three plantations, UAS-derived tree densities were lower than ground-based estimates, likely due to overlapping of tree crowns limiting detection of trees in lower canopy positions. The remaining four plantations with relatively lower ground-derived tree densities (02_002, 07_011, 07_012, and 10_001) were associated with comparatively more accurate UAS-derived estimates of tree density using optimized window parameters (Table 6). Furthermore, the necessity for calibrating optimal window parameters to derive accurate tree density estimates and additional structural metrics is underscored in the case of stand 10_001. With a relatively lower tree density of 178 trees per hectare (72 trees per acre) compared to other plantations, using 3 m, circular windows resulted in an overestimation of 173 trees per hectare (Table 4) from UAS-derived metrics likely due to multiple local maxima detected within the same tree crown. However, increasing the window size to 5 m reduced the absolute error of UAS-derived tree density to 10 trees per hectare (Table 6). Individual tree detection accuracy using local maxima filtering is considered a function of crown diameter, with a window size smaller than the average crown diameter resulting in the commission of treetops, while window sizes larger than the average crown diameter resulting in the omission of treetops (Wulder et al. 2000).With a plantation level average crown diameter of 4.7 m, a window size of 5 m was closer to the average crown diameter than a window size of 3 m. Ultimately, in less dense stands, less than 200 trees per hectare, larger window sizes closely related to average crown diameter should be employed, whereas smaller window sizes should be employed in denser stands, more than 200 trees per hectare, under leaf-on conditions. Furthermore, acquiring leaf-off and leaf-on imagery may allow for better individual tree detection through more accurate DTM (Nasiri et al. 2021). Use of rasterized CHM, rather than normalized point cloud, with smoothing functions may also allow for reduction of commission of treetops, especially when DTMs are generated from leaf-off imagery, and therefore better detect number of trees per plantation (Nasiri et al. 2021).

With an overall mean absolute error of 0.5 m, plantation level canopy height was the most accurate metric in relation to ground-based inventory. Due to the limited ability of imaging technology to provide sufficient canopy penetration under dense conditions to generate an accurate digital terrain model, the derivation of canopy height relied heavily on the manual re-classification of erroneously classified ground points from which the heights of above ground points could be interpolated. Despite some underestimations of tree density at the plantation level, it appears that estimates of canopy height were marginally affected. At the plot level, however, absolute errors of canopy height had an overall mean absolute error of 1.4 m. As the accuracy of additional structural metrics relies on the accurate detection of individual trees from which those metrics can be derived, the fact that plantation level estimates of canopy height were more accurate than those at the plot level is not surprising. At the plantation level, it is likely that larger tree sample size resulted in more normal distribution of heights and a closer estimate of the overall mean canopy height to ground measurements.

UAS-derived canopy cover overestimated ground-based cover by 16.7%, ranging from 2 to 24%. This may be the result of imaging technology's limited ability to penetrate through small canopy gaps and discern between homogenous, overlapping crowns, ultimately resulting in an overestimation of total crown area (Koch et al. 2006; Wallace et al. 2016). This overlooking of small gaps among trees would have inflated canopy cover compared to canopy cover determined from tree crown projection areas calculated from ground-based inventory. Regardless, UAS-derived canopy cover estimates are useful for describing hardwood plantation conditions and management needs as part of a monitoring scheme for wetland reserve easements, especially for applications that require precision levels congruent with the mean absolute errors reported here such attainment of canopy closure. Albeit it is important to recognize the potential for misclassifying plantations on the margins of target ranges and use a correction factor to ensure greater agreement with ground-derived canopy cover estimates.

UAS-SfM was found to be a viable method for assessing canopy height and percent cover of WRP hardwood plantations, with the accuracy of tree density estimates relying upon the selected local maxima window parameters. Furthermore, for canopy height and cover estimates to be within an acceptable range relative to ground-based measurements, it is recommended that plantation conditions are used to calibrate local maxima parameters. In general, local maxima parameters may be calibrated with a subset of ground-based data and applied at the plantation level. Ultimately, using a subset of ground data to calibrate local maxima parameters should allow for more accurate tree density and canopy cover estimates, with a reduction in time and resources compared to traditional ground-based inventory methods. Collection of leaf-off imagery (Nasiri et al. 2021) and capture of tree stem surfaces (Kuželka and Surový 2018) would extend SfM capability to providing additional forest monitoring requirements such as tree diameter, stocking, and canopy gaps. Furthermore, UAS-captured, LiDAR-derived point clouds may offer improved estimates of tree density due to the enhanced ability to penetrate forest canopies compared to UAS-SfM technology (Wallace et al. 2016).

In addition to exploring alternative approaches to automated individual tree detection, future research should focus on analyzing bottomland hardwood species-specific height to crown diameter relationships. Models of these relationships can be used to employ more accurate and robust variable window size functions, without additional ground data, in which window size varies as a function of tree height so that it is more accurately related to crown diameter. Furthermore, since spatial positions of reference trees were not collected, omission/commission errors associated with various window parameters were not quantified. Considering this limitation, it was not possible to determine the spatial accuracy of the UAS-detected treetops in this study and only overall tree density estimates were compared to ground-based measurements. Additionally, imagery captured under leaf-off conditions may facilitate more accurate tree density estimates due to more accurate classification of ground points and their corresponding interpolated surfaces needed in the height normalization step (Nasiri et al. 2021).

Supplementary Information The online version contains supplementary material available at https://doi.org/10.1007/s13157-024-01807-6.

Acknowledgements Thanks to all students that participated in field data collection, especially James Borland. Special thanks to John Dennis for assistance, consulting on data collection, and conducting some of the flights used in this study.
Statements and Declarations.

Author Contributions Conceptualization, M.B.; methodology, T.C. and M.B.; software, T.C. and M.B.; validation, T.C. and M.B.; formal analysis, T.C.; investigation, T.C. and M.B.; resources, M.B.; data curation, M.B.; writing—original draft preparation, T.C.; writing—review and editing, T.C. and M.B.; visualization, T.C. and M.B.; supervision, M.B.; project administration, M.B.; funding acquisition, M.B. All authors have read and agreed to the published version of the manuscript.

Funding This research was funded by the Natural Resources Conservation Service-Arkansas under funding opportunity number USDA-NRCS-AR-17-01 and grant 68-7103-17-114 with partial funding provided by the McIntire-Stennis Cooperative Forestry Research Program (project no. 1023834- ARK02681). Support for the Article Processing Charge was provided by the U.S. Forest Service Southern Research Station Center for Forest Health and Disturbance—Research Work Unit 4552 Insects, Diseases, and Invasive Plants.

Data Availability All data generated or analyzed during this study are included in this published article. Access to datasets used and/or analyzed is available from the corresponding author on reasonable request.

Declarations

Competing Interests The authors have no relevant financial or non-financial interests to disclose.

References

Berkowitz JF (2013) Development of restoration trajectory metrics in reforested bottomland hardwood forests applying a rapid assessment approach. Ecol Ind 34:600–606

De Steven D, Faulkner SP, Keeland BD, Baldwin MJ, McCoy JW, Hughes SC (2015) Understory vegetation as an indicator for floodplain forest restoration in the Mississippi River Alluvial Valley, USA. Restor Ecol 23:402–412

Falkowski MJ, Smith AM, Gessler PE, Hudak AT, Vierling LA, Evans JS (2008) The influence of conifer forest canopy cover on the accuracy of two individual tree measurement algorithms using lidar data. Can J Remote Sens 34:1–13

Gebreslasie M, Ahmed F, van Aardt JA (2009) Image-based reflectance conversion of ASTER and IKONOS imagery as precursor to structural assessment of plantation forests in KwaZulu-Natal, South Africa. South Forests 71:259–265

Iglhaut J, Cabo C, Puliti S, Piermattei L, O'Connor J, Rosette J (2019) Structure from motion photogrammetry in forestry: a review. Curr Forestry Rep 5:155–168

Jayathunga S, Owari T, Tsuyuki S (2018) Evaluating the performance of photogrammetric products using fixed-wing UAV imagery over a mixed conifer–broadleaf forest: comparison with airborne laser scanning. Remote Sens 10:187

Ke Y, Quackenbush LJ (2011) A review of methods for automatic individual tree-crown detection and delineation from passive remote sensing. Int J Remote Sens 32:4725–4747

King SL, Keeland BD (1999) Evaluation of reforestation in the lower Mississippi River Alluvial Valley. Restor Ecol 7:348–359

Klimas C, Murray E, Foti T, Pagan J, Williamson M, Langston H (2009) An ecosystem restoration model for the Mississippi Alluvial Valley based on geomorphology, soils, and hydrology. Wetlands 29:430–450

Koch B, Heyder U, Weinacker H (2006) Detection of individual tree crowns in airborne lidar data. Photogrammetric Eng Remote Sens 72:357–363

Kuželka K, Surový P (2018) Mapping forest structure using UAS inside flight capabilities. Sensors 18:1–13

LMVJV (2007) In: Wilson R, Ribbeck K, King S, Twedt D (eds) Restoration, management, and monitoring of forest resources in the Mississippi Alluvial Valley: recommendations for enhancing wildlife habitat. Forest Resource Conservation Working Group Lower Mississippi Valley Joint Venture, Vicksburg, MS, pp 1–98

Marcaccio JV, Markle CE, Chow-Fraser P (2015) Unmanned aerial vehicles produce high-resolution, seasonally-relevant imagery for classifying wetland vegetation. Int Archives Photogrammetry Remote Sens Spat Inform Sci 40:249–256

Maturbongs B, Wing M, Strimbu B, Burnett J (2019) Forest inventory sensitivity to UAS-based image processing algorithms. Annals for Res 62:87–108

Mohan M, Leite RV, Broadbent EN, Wan Mohd Jaafar WS, Srinivasan S, Bajaj S, Dalla Corte AP, do Amaral CH, Gopan G, Saad SNM, Kamarulzaman AMM, Prata GA, Llewelyn E, Johnson DJ, Doaemo W, Bohlman S, Zambrano AMA, Cardil A (2021) Individual tree detection using UAV-lidar and UAV-SfM data: a tutorial for beginners. Open Geosci 13:1028–1039

Nasiri V, Darvishsefat AA, Arefi H, Pierrot-Deseilligny M, Namiranian M, Le Bris A (2021) Unmanned aerial vehicles (UAV)-based canopy height modeling under leaf-on and leaf-off conditions for determining tree height and crown diameter (case study: hyrcanian mixed forest). Can J for Res 51:962–971

NRCS (2023) Restoring America's Wetlands: Agricultural Conservation Easement Program. pp. 1–8. In N. R. C. S. USDA (ed.), Online

Popescu SC, Wynne RH (2004) Seeing the trees in the forest: using lidar and multispectral data fusion with local filtering and variable window size for estimating tree height. Photogrammetric Eng Remote Sens 70:589–604

RCoreTeam (2023) R: a language and environment for statistical computing. R Foundation for Statistical Computing, Vienna, Austria

Roussel J-R, Goodbody T, Tompalski P (2023) The lidR package

Tao W, Lei Y, Mooney P (2011) Dense point cloud extraction from UAV captured images in forest area. pp. 389–392. Proceedings 2011 IEEE International Conference on Spatial Data Mining and Geographical Knowledge Services. Ieee

Tomaštík J, Mokroš M, Surový P, Grznárová A, Merganič J (2019) UAV RTK/PPK method—an optimal solution for mapping inaccessible forested areas? Remote Sens 11:1–19

Walbridge MR (1993) Functions and values of forested wetlands in the southern United States. J Forest 91:15–19

Wallace L, Lucieer A, Malenovský Z, Turner D, Vopěnka P (2016) Assessment of forest structure using two UAV techniques: a comparison of airborne laser scanning and structure from motion (SfM) point clouds. Forests 7:1–16

Wulder M, Niemann KO, Goodenough DG (2000) Local maximum filtering for the extraction of tree locations and basal area from high spatial resolution imagery. Remote Sens Environ 73:103–114

Zhang J, Virk S, Porter W, Kenworthy K, Sullivan D, Schwartz B (2019) Applications of unmanned aerial vehicle based imagery in turfgrass field trials. Front Plant Sci 10:1–12

Zhen Z, Quackenbush LJ, Zhang L (2016) Trends in automatic individual tree crown detection and delineation—evolution of LiDAR data. Remote Sens 8:1–26